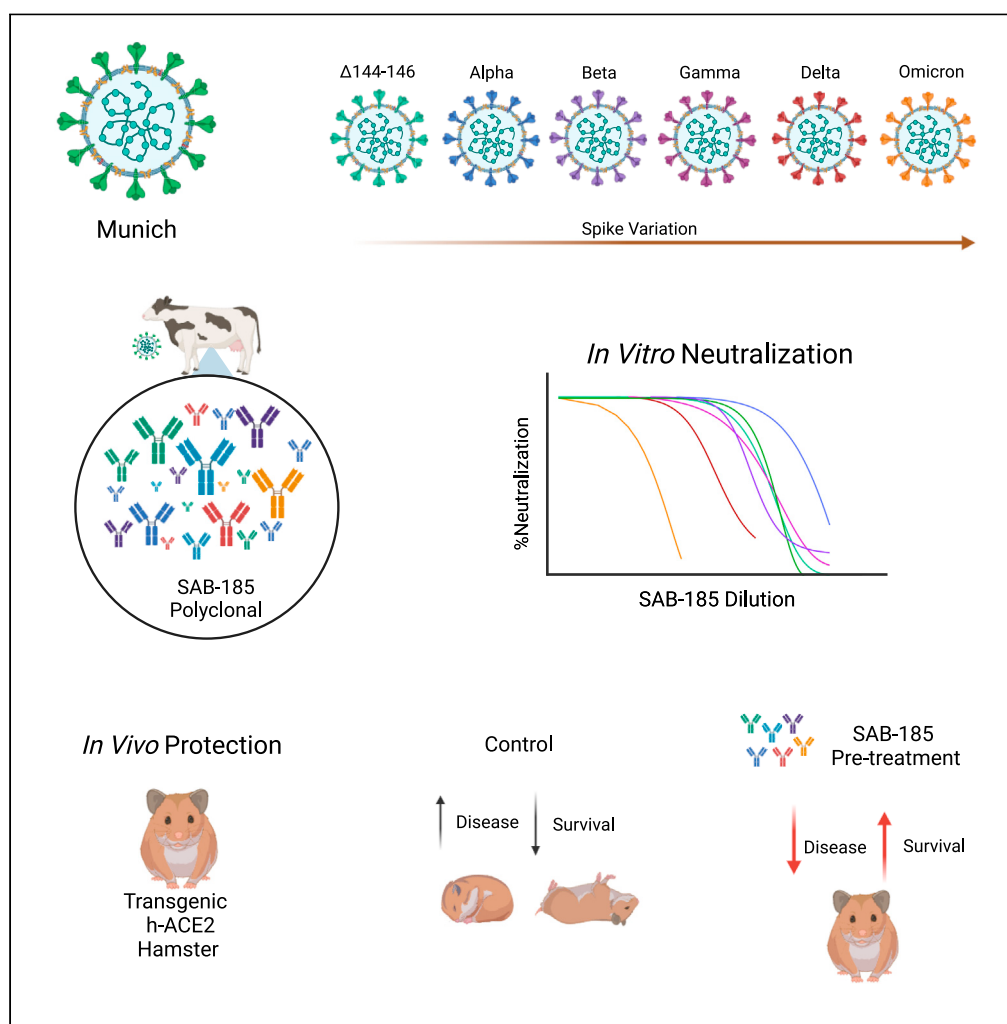


Article

Transchromosomal bovine-derived anti-SARS-CoV-2 polyclonal human antibodies protects hACE2 transgenic hamsters against multiple variants



Theron Gilliland,
Matthew Dunn,
Yanan Liu, ...,
Eddie Sullivan,
Zhongde Wang,
William B. Klimstra

klimstra@pitt.edu

Highlights

A transchromosomal bovine polyclonal antibody neutralizes variants of SARS-CoV-2

We use a novel human ACE2 (hACE2) transgenic hamster model of SARS-CoV-2 infection

The polyclonal antibody protects hACE2 hamsters from all variants tested

Hyperimmunization of the bovines may promote protection against SARS-CoV-2 variants

Gilliland et al., iScience 26, 107764
October 20, 2023 © 2023 The Authors.
<https://doi.org/10.1016/j.isci.2023.107764>



Article

Transchromosomal bovine-derived anti-SARS-CoV-2 polyclonal human antibodies protects hACE2 transgenic hamsters against multiple variants

Theron Gilliland,^{1,5} Matthew Dunn,^{1,5} Yanan Liu,^{3,5} Maria D.H. Alcorn,¹ Yutaka Terada,¹ Shauna Vasilatos,¹ Jeneveve Lundy,¹ Rong Li,³ Sham Nambulli,² Deanna Larson,³ Paul Duprex,² Hua Wu,⁴ Thomas Luke,⁴ Christoph Bausch,⁴ Kristi Eglund,⁴ Eddie Sullivan,⁴ Zhongde Wang,³ and William B. Klimstra^{1,6,*}

SUMMARY

Pandemic SARS-CoV-2 has undergone rapid evolution resulting in the emergence of many variants with mutations in the spike protein, some of which appear to evade antibody neutralization, transmit more efficiently, and/or exhibit altered virulence. This raises significant concerns regarding the efficacy of anti-S monoclonal antibody-based therapeutics which have failed against variant SARS-CoV-2 viruses. To address this concern, SAB-185, a human anti-SARS-CoV-2 polyclonal antibody was generated in the DiversitAb platform. SAB-185 exhibited equivalent, robust *in vitro* neutralization for Munich, Alpha, Beta, Gamma, and Δ 144-146 variants and, although diminished, retained PRNT₅₀ and PRNT₈₀ neutralization endpoints for Delta and Omicron variants. Human ACE2 transgenic Syrian hamsters, which exhibit lethal SARS-CoV-2 disease, were protected from mortality after challenge with the Munich, Alpha, Beta, Delta, and Δ 144-146 variants and clinical signs after non-lethal Omicron BA.1 infection. This suggests that SAB-185 may be an effective immunotherapy even in the presence of ongoing viral mutation.

INTRODUCTION

SARS-CoV-2 has spread worldwide during the previous two years resulting in over 600 million cases and over 6 million deaths (WHO dashboard <https://covid19.who.int>).¹ Since late fall 2020, variant viruses have been identified that exhibit altered infection, transmission, and disease characteristics,^{2,3} as reviewed earlier.⁴⁻⁷ These variants may reflect immune response escape mutants as well as mutants adapting to replication and transmission in normal or immunocompromised human populations⁸⁻¹⁰; reviewed by Gomez et al. and Peacock et al.^{11,12} Of particular concern are variants with multiple changes in the spike protein, which is a primary target of acquired immune responses. These mutated viruses exhibit increased resistance to spike-targeted vaccines and immuno-therapeutics such as monoclonal antibodies,^{8,9,13-16} as reviewed earlier.^{2,17-19}

To address the need for improved pathogen immunotherapies, SAB Biotherapeutics, Inc. (SAB) created the DiversitAb platform that utilizes vaccination of transchromosomal (Tc) bovine to produce diverse, fully human pAbs.²⁰⁻²⁵ We have previously demonstrated the pre-clinical efficacy of this platform against Middle East respiratory syndrome coronavirus (MERS-CoV), Ebola, and Venezuelan equine encephalitis viruses, among others.²³⁻²⁵ In separate studies with SARS-CoV-2, SAB-185 exhibited *in vitro* neutralization of the SARS CoV-2 (Munich/D614G variant), several VSV-SARS-CoV-2 pseudotyped chimeric virus variants and prevented the identification/development of escape variants as compared to a monoclonal antibody.²⁶ Here, we demonstrate that SAB-185 retains *in vitro* neutralization of ten SARS-CoV-2 variants and show the *in vivo* protective efficacy against six SARS-CoV-2 variants using a new human ACE2 receptor transgenic hamster model.²⁷

RESULTS

Neutralization of SARS-CoV-2 variants by SAB 185 *in vitro*

The generation, purification, and characterization of SAB-185 have been previously described.²⁸ Here, we evaluated the ability of SAB-185 to neutralize a panel of SARS-CoV-2 variants by plaque assay with Vero E6 or Vero Ace2/TMPRSS2 (Vero A/T) cells (Figure 1A and 1B). SAB-185

¹Center for Vaccine Research and Department of Immunology, University of Pittsburgh, Pittsburgh, PA 15261, USA

²Center for Vaccine Research and Department of Microbiology and Molecular Genetics, University of Pittsburgh, Pittsburgh, PA 15261, USA

³Department of Animal Dairy, Veterinary Sciences, Utah State University, Logan, UT 84341, USA

⁴SAB Biotherapeutics, Inc, Sioux Falls, SD 57104, USA

⁵These authors contributed equally

⁶Lead contact

*Correspondence: klimstra@pitt.edu

<https://doi.org/10.1016/j.isci.2023.107764>



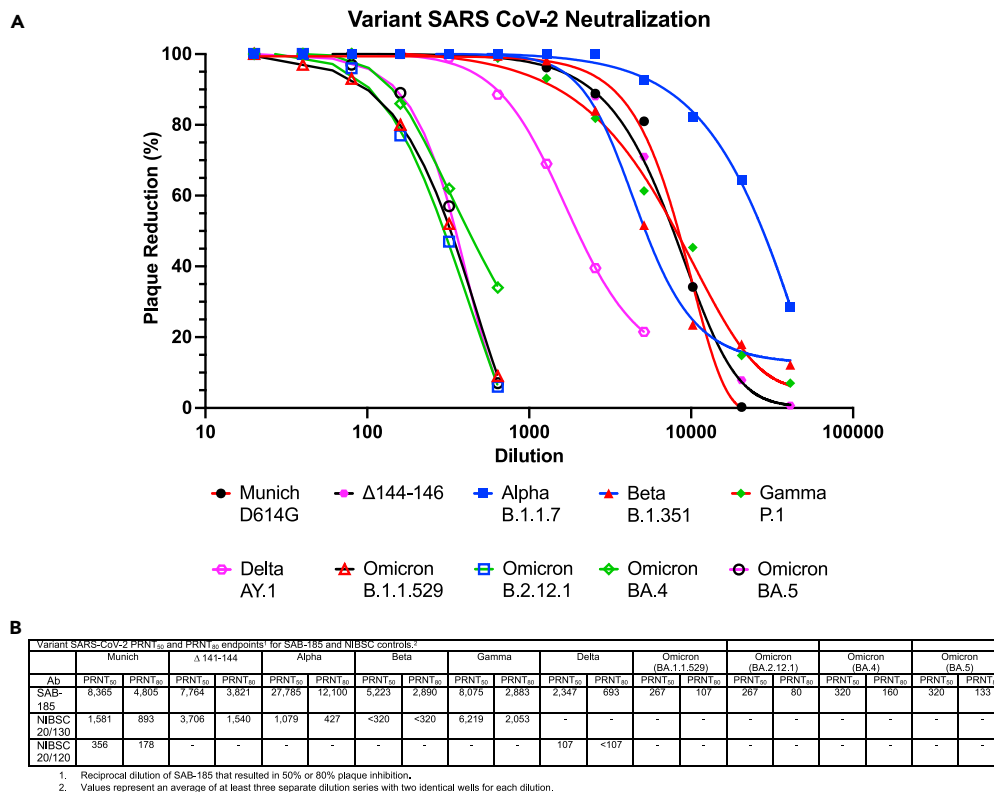


Figure 1. SAB-185 neutralization potential versus the Munich variant (spike D614G) and other variants

(A) Nonlinear curve fits to dilution versus plaque inhibition data.

(B) Calculated PRNT50 and PRNT80 endpoints. Neutralization capacity of SAB-185 and the NIBSC controls was assayed by Vero E6 or Vero hACE2/TMPRSS2 cell plaque neutralization assay. SAB-185 was diluted to 1 mg/ml in PBS and then diluted serially 2-fold before reaction with viruses. NIBSC controls were diluted 2-fold and then 2-fold serially. Data points are averages of results from at least 3 replicates with 2 averaged duplicate wells at each dilution. Error bars are omitted for clarity.

neutralized the Munich, Alpha, Beta, Gamma, and Δ 144-146 variants equivalently on Vero E6 cells with PRNT₅₀ values ranging from 1:5,223 to 1:27,785. SAB-185 neutralized the Delta variant AY.1 and Omicron BA.1.1.529 variants with a ~4-fold and 31-fold respective average decrease versus Munich. In comparison, a National Institute for Biological Standards and Control convalescent human serum (NIBSC 20/130) neutralized the Munich, Alpha, Δ 144-146, and Gamma variants (PRNT₅₀ range 1:1,079-1:6,219) but failed to provide 50% neutralization against the Beta variant at a 1:320 dilution. Similarly, the NIBSC 20/120 control showed a decrease between the Munich (PRNT₅₀ 1:356) and Delta (PRNT₅₀ 1:107) variants (Figure 1B). NIBSC controls were not available for the Gamma and Omicron neutralization assays.

The Syrian hamster was among the first rodents to be used as a model to study SARS-CoV-2 infection. Normal hamsters are susceptible to SARS-CoV-2 infection but only develop mild clinical disease limiting their utility to assess vaccine and therapeutic efficacy.²⁹ We first evaluated the ability of SAB185 to protect normal Syrian hamsters from weight loss and clinical signs with the Munich strain infection as the disease in these animals is not fatal. Significant protection from both was observed at multiple times post infection (Figure S1). While the hamster ACE2 protein (hACE2) serves as a functional cell receptor for SARS-CoV-2 infection, some amino acid residues that are critical for the recognition and binding by the SARS-CoV-2 spike protein are not conserved between the hamster ACE2 and human ACE2 protein, possibly diminishing infectivity of SARS-CoV-2 in the hamster model.^{30,31} To develop a highly susceptible hamster model capable of mimicking severe/fatal infection in humans, we employed a piggyBac-mediated transgenic approach and generated multiple independent hACE2 transgenic hamster lines expressing the human ACE2 gene from the human cytokeratin 18 promoter used previously to create hACE2-expressing mice.^{32,33} These hamster lines are highly susceptible to SARS-CoV-2 infection via intranasal infection and develop respiratory disease and mortality, similar to that observed in severe COVID-19 patients.³²

SAB 185 protection of hACE2 hamsters from mortality

We initially evaluated the disease course after intratracheal (it.) versus intranasal (in.) infection of hACE2 animals. Significant differences in survival time or weight loss were not observed with the exception of a single animal surviving the it. infection (Figure S2, day 6 single it. animal). We chose to determine the protective efficacy of SAB-185 after it. rather than in. infection to minimize direct infection of the CNS through the olfactory neuroepithelium. SAB-185 (50 mg/kg), or an equivalent volume of PBS for control groups, was delivered via intramuscular injection in

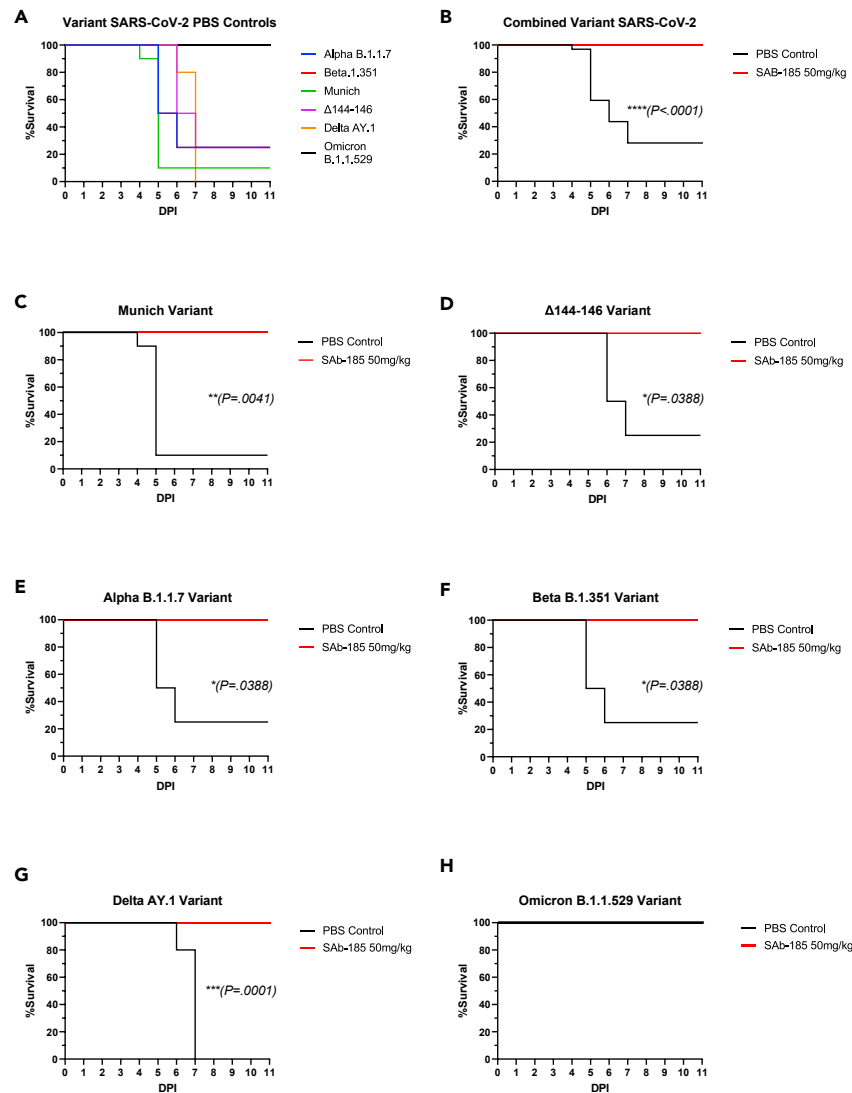


Figure 2. SAB-185 protection from mortality in hamsters challenged with six variant SARS-CoV-2 isolates

(A–H) Hamsters were administered SAB-185 or PBS intramuscularly and then challenged intratracheally 24 h later with 1000 plaque-forming units of variant virus. Mortality for individual variant PBS controls (A) and for combined (all SARS-CoV-2 variants tested) PBS control versus SAB-185-treated groups (B). Individual mortality data for Munich (C), Δ 144-146 (D) Alpha (E), Beta (F), Delta (G), and Omicron (H) viruses. Mantel-Cox log rank significance is indicated within each panel. * $p < 0.05$, ** $p < 0.01$, *** $p < 0.005$.

the gastrocnemius muscle followed 24 h later by its challenge with \sim 1000 Vero E6 plaque-forming units of each variant virus. A sex-based difference was observed in control groups challenged with Munich, Alpha, Beta, Gamma, Delta, and Δ 144-146 variants as all female animals died between four- and seven-days post infection and male hamsters exhibited 50 to 100% mortality over a similar interval (data not shown). Mortality curves were not significantly different between the Munich and Δ 144-146, Alpha, Beta, Gamma, or Delta SARS CoV-2 variants (Figure 2A) (variants compared to Munich: $p > 0.05$).

SAB-185 treatment prior to infection completely protected all hamsters from death, regardless of sex, when challenged with Munich, Δ 144-146, Alpha, Beta, and Delta variants (Figures 2B–2G). In animals challenged with the Omicron variant, mortality was not observed (Figure 1H). However, as described in detail in the following text, weight loss and clinical signs of disease were observed in untreated hamsters, similar to a published report assessing the virulence of Omicron following intranasal infection using hACE2 hamsters.³⁴

SAB-185 protection of hACE2 hamsters from weight loss

In addition to mortality, hamsters were also assessed daily for signs of disease, such as weight loss (Figure 3) and clinical scoring (see, Figure 4). Without treatment, hACE2 hamsters challenged with Munich, Δ 144-146, Alpha, Beta, and Delta variants experienced weight loss beginning

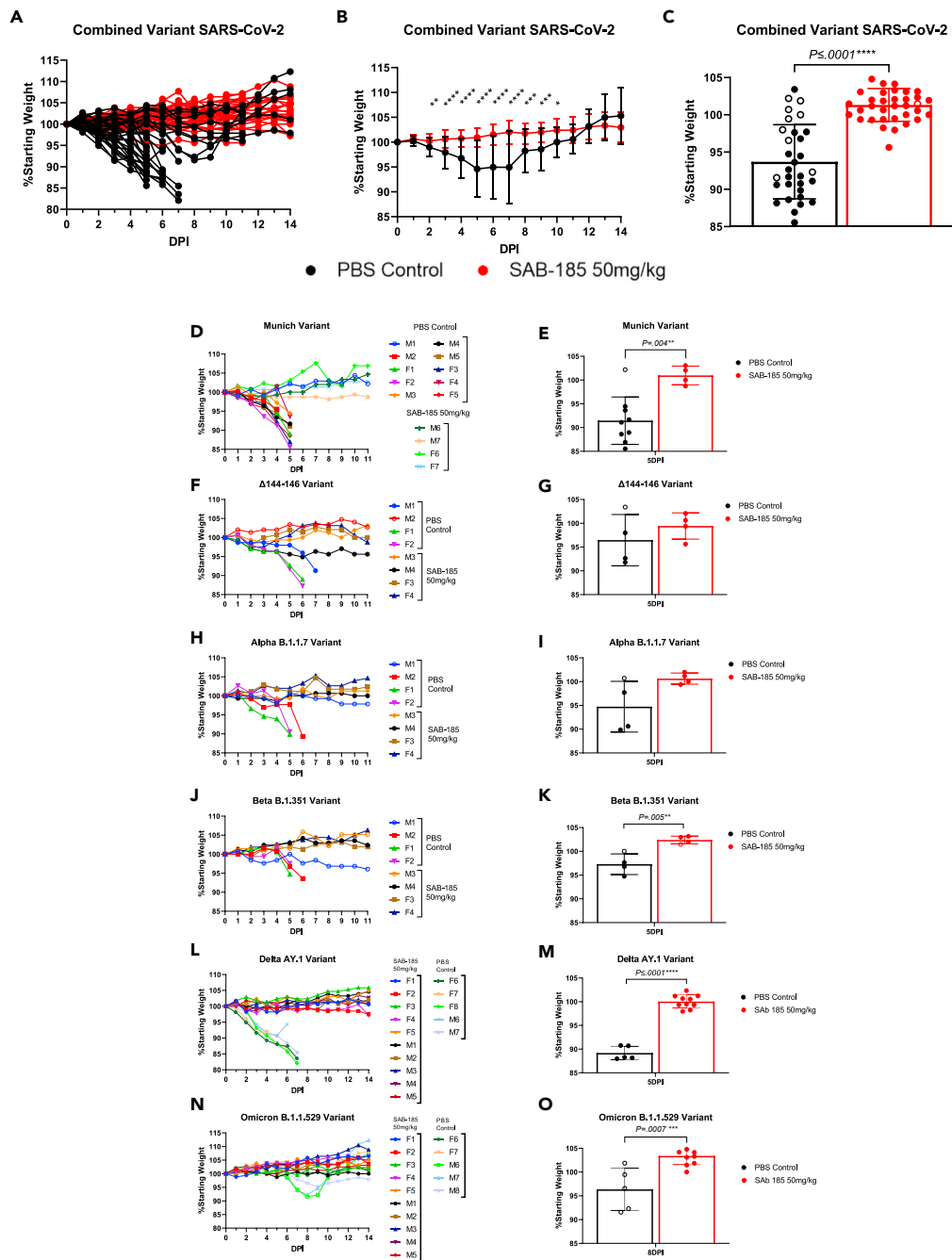


Figure 3. SAB-185 protection from weight loss in hamsters challenged with six variant SARS-CoV-2 isolates

(A) Weight loss for individual hamsters in all groups.

(B) Combined (all SARS-CoV-2 variants tested) average weight loss data for SAB-185-treated and PBS control hamsters.

(C) Combined average weight loss data for SAB-185-treated and PBS control hamsters on D5 (last day all animals were alive) or D8 post challenge for Omicron-infected animals (peak clinical signs).

(D–O) Individual weight loss data for Munich (D), Δ144-146 (F), Alpha (H), Beta (J), Delta (L) and Omicron (N) viruses. Combined average weight loss data for Munich (E), Δ144-146 (G), Alpha (I), Beta (K) and Delta (M) variants on D5 (last day all animals were alive) post challenge or D8 post challenge for Omicron-infected animals (O) (peak weight loss). * $p < 0.05$, ** $p < 0.01$, *** $p < 0.005$. Open circles are surviving animals (controls) and the SAB-185 treated animal that exhibited delayed replication.

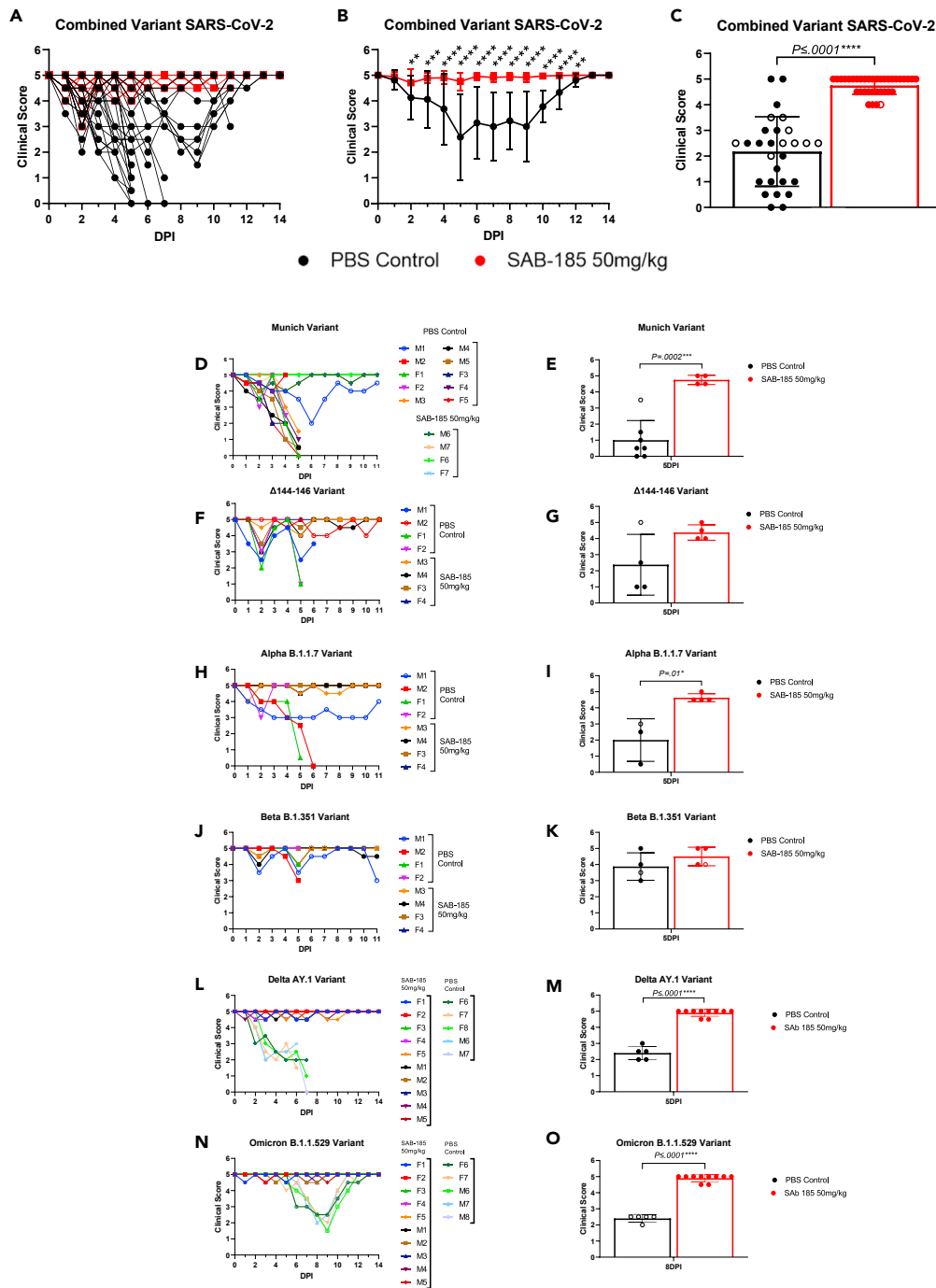


Figure 4. SAB-185 protection from clinical signs in hamsters challenged with six variant SARS-CoV-2 isolates

Data is presented as the inverse of the clinical score sum values, as described in Materials and Methods, to be comparable to weight loss data. Each datum point represents an average of morning and afternoon observations.

(A) Clinical sign scoring for individual hamsters in all groups. Each datum point represents an average of morning and afternoon observations.

(B) Combined clinical sign scoring data for SAB-185-treated and control hamsters.

(C) Combined clinical sign scoring data for SAB-185-treated and control hamsters on D5 (last day all animals were alive) post challenge or D8 post challenge for Omicron-infected animals (peak clinical signs).

Figure 4. Continued

(D–O) (B) Individual clinical sign scoring data for Munich (D), Δ 144-146 (F) Alpha (H), Beta (J), Delta (L) and Omicron (N) viruses. Individual clinical sign scoring data for Munich (E), Δ 144-146 (G) UK (I), SA (K), Delta (M), and Omicron (O) variants on D5 (last day all animals were alive) post challenge or D8 post challenge for Omicron (peak clinical signs). * $p < 0.05$, ** $p < 0.01$, *** $p < 0.005$. Open circles are surviving (controls and Omicron) and the SAB-185 treated animal that exhibited delayed replication.

between D1 and D2 post challenge with peak weight loss between D5 and D7, depending upon the variant. Hamsters challenged with Omicron experienced weight loss beginning on day 6 with peak weight loss on day 8. When treated with SAB-185 prior to variant virus challenge, the hamsters, on average, did not lose weight and weight loss was significantly greater in PBS controls on D2-11 post challenge (Figure 3B). The greatest difference in weight was observed on D5 for Munich, Δ 144-146, Alpha, Beta, Delta variants, the last day on which all animals were alive (Figures 3D–3M), and D8 for Omicron, the day of peak disease (Figures 3C, 3N, and 3O). When each group was analyzed individually, hamsters treated with SAB-185 and challenged with Munich, Beta, Delta, and Omicron variants exhibited significantly less weight loss than PBS controls (Figures 3E, 3K, 3M, and 3O). While hamsters in the PBS control groups challenged with Alpha and Δ 144-146 variants experienced weight loss, the difference failed to reach statistical significance compared to SAB-185-treated hamsters challenged with the same variants (Figures 3F–3I). Interestingly, the only surviving PBS control male that did not lose weight over the course of the experiment was in the Alpha challenge group (Figure 3H), suggesting this animal's infection was limited. Additionally, the only SAB-185 treated animal to lose weight was in the Δ 144-146 group (Figure 3F), and this animal survived infection. If survivors in the PBS control groups and the poorly infected SAB-185-treated animal were removed, D5 weight loss was significantly lower for Alpha and Beta infected SAB-185 treated animals (Figures S3D, S3F, and S3G), and the significance of Munich differences increased. The SAB-185 treated, Δ 144-146 challenged animals exhibited a non-significant trend toward less weight loss by D5 (Figure S3E).

SAB-185 protection of hACE2 hamsters from clinical signs

In addition to daily weights, hamsters were evaluated twice daily for clinical signs of disease (ruffled fur, hunching, increased respiratory rate, anorexia, and lethargy) (Figure 4). In concordance with the mortality and weight loss data, PBS control hamsters challenged with Munich, Alpha, Beta, Delta, and Δ 144-146 variants showed signs of infection starting on D1 to D2 with a peak on D5 post challenge (Figure 4A–4M). Challenge with the Omicron variant caused delayed signs of infection, with clinical signs of disease beginning on days 5–6 with peak disease occurring on days 8–9, (Figure 4N and 4O). When combining the SARS-CoV variant groups, clinical signs were significantly lower in PBS controls compared to the SAB-185-treatment group on D2-12 (Figure 4B) and highly significant ($p < 0.001$) on D4-12 (Figures 4B and 4C). When analyzed individually, SAB-185 treatment significantly reduced signs of disease in animals challenged with Munich, Alpha, Delta, and Omicron (Figures 4E, 4I, 4M, and 4O). The average clinical score for PBS control animals challenged with Δ 144-146 and Beta was lower compared to SAB-185-treated animals in these groups but did not reach statistical significance (Figures 4G and 4K). However, if PBS control survivors and the poorly infected SAB-185 animal were removed, the SAB-185-treated animals were also significantly different (Figure S4). While mortality was observed, clinical signs were less severe in control animals challenged with the Beta virus versus the other variants (Figures 4D, 4F, 4H, 4J, 4L, and 4N), which could attribute to the smaller treated versus control differences with this strain.

Effect of SAB-185 treatment on SARS-CoV-2 oropharyngeal plaque and PCR titers

Lastly, we assessed viral titers in oropharyngeal swabs taken from animals every other day starting on D1 or D2 and continuing through D10 or D11 post challenge. Swabs were assayed for virus genome equivalents (GE) by quantitative RT-PCR (Figure S5) and plaque assay. GE titers in control animals ranged from undetectable (250 GE limit of detection) to greater than 1×10^7 GE/mL on D1-2 post challenge (Figure S5). Titers were highly variable between individual animals between combined control and SAB-185-treatment groups (Figures S5A–S5C) and none of the titers were significantly different ($p > 0.05$) (Figures S5B and S5C). Notably, undetectable titers on D3-5 were associated with survival of the male animals in Munich, Δ 144-146, Alpha, and Beta control groups. However, titers in all surviving animals had risen to detectable levels by D6 (Figures S5D, S5F, S5H, and S5J). Only one animal in the SAB-185-treated group exhibited this replication profile (Beta variant challenge group Figure S5J), suggesting that only one of the SAB-185 animals might have survived without pAb treatment. As noted in weight loss and clinical sign sections previously, if samples without titer on D3 to 5 were omitted from the analyses (this includes the 4 surviving controls and one challenged SAB-185-treated animal, Figures S4A–S4G), the combined data show a non-significant trend toward lower virus genome titers on D5 (Figure S6C) with SAB-185 treatment. Non-significant trends toward lower genome abundance were also observed in Alpha and Beta SAB-185-treatment groups (Figures S6F and S6G). Oropharyngeal swab plaque titers for all hamsters were below the limit of detection of a plaque assay (25 PFU/mL) on all measured days post challenge, which suggests that genomic RNA detected by the PCR assay was not associated with shedding of high levels of live virus.

DISCUSSION

The occurrence of successive waves of SARS-CoV-2 variants with novel spike-protein mutations throughout the COVID-19 pandemic has reduced the prophylactic efficacy of vaccines^{9,10,12} and abrogated the efficacy of many antibody-based therapeutics¹⁶. SAB-185 is a human polyclonal IgG generated in the DiversitAb platform produced using spike protein from the WA-1 SARS CoV-2 variant. The current studies demonstrated that a single IM injection of SAB-185 protected recombinant hACE2 hamsters from mortality and/or severe morbidity when

intratracheally infected with successive SARS CoV-2 variants including Omicron. Although reduced *in vitro* SAB-185 PRNT₅₀ and PRNT₈₀ neutralization titers were observed with Delta and Omicron variants, the preparation still was highly protective at human-relevant doses *in vivo*. Therefore, reduced *in vitro* neutralization titers of SAB-185 against SARS CoV-2 variants were not associated with loss of *in vivo* efficacy.

The hACE2 transgenic hamsters used here provide a new and relevant model of severe/fatal SARS CoV-2 disease that can be utilized to test future vaccines and therapeutics.³² Consistent with other studies using normal hamsters and other animal models and possibly human infections,^{35–38} mild versus severe manifestations of disease were not closely associated with an effect on oropharyngeal swab GE titers. However, if control and SAB-185-treated animals that had delayed virus replication were removed, suppression of titers by SAB-185 was significant for combined challenge groups ($p = 0.01$). Furthermore, high-GE titers in oropharyngeal secretions were not associated with detectable live virus, suggesting that the GE shedding may not be productive for transmission. These data contribute to the body of evidence that vaccination and/or Ab therapeutic treatment may only provide limited protection from virus infection and upper respiratory tract replication while reducing severe disease.

Reasons underlying the protective efficacy of SAB-185 versus multiple strains may include the hyper-immunization of Tc bovines with full-length spike pDNA for priming and recombinant spike ectodomain protein for boosting, which may increase stimulation of polyclonal antibodies reactive with subdominant epitopes that are less likely/able to mutate during widespread human infection. Loss of reactivity of monoclonal antibodies that bind various epitopes in the S protein has been demonstrated clearly,^{16,8,39,40} and the broad reactivity provided by polyclonal Ab products may have an advantage in neutralization and protection against variants. In addition, other factors such as non-neutralizing anti-spike antibodies and/or innate immune mechanisms such as effector cell function(s) that were previously reported in an anti-Ebola immunoglobulin produced in the DiversitAb platform²³ could be important *in vivo*.

In summary, the DiversitAb platform represents a highly scalable system that produces high-neutralizing titer, fully human polyclonal antibodies. SAB-185 retained neutralization activity against successive SARS-CoV-2 variants, and this was associated with protection from mortality and/or severe disease in the hACE2 hamster model. The data in this report suggests that human anti-SARS-CoV-2 polyclonal antibody, SAB-185, may have broad efficacy in preventing or treating SARS-CoV-2 variant infections in humans. This will need to be confirmed in human clinical trials. Such trials could include studies in severely immuno-compromised patients that are known to manifest severe disease, prolonged viral replication, and the ability to produce SARS CoV-2 variants such as the spike $\Delta 144-146$ variant used in this study.

Limitations of the study

While SAB-185 was protective from SARS-CoV-2 mortality and clinical signs in the lethal hACE2 hamster model, it is unclear how this might translate to treatment of human patients infected with SARS CoV-2. The route of infection used here may not mimic the route of infection in humans and, therefore, the antibodies in SAB-185 may not have similar exposure to circulating virions or infected cells. Furthermore, it is unlikely that most treatment of humans would occur prior to exposure to SARS-CoV-2. Further research is required to determine the relationship of SAB-185 efficacy to timing of treatment relative to virus infection.

STAR★METHODS

Detailed methods are provided in the online version of this paper and include the following:

- KEY RESOURCES TABLE
- RESOURCE AVAILABILITY
 - Lead contact
 - Materials availability
 - Data and code availability
- EXPERIMENTAL MODEL AND STUDY PARTICIPANTS DETAILS
 - Animals
 - Viral stocks
 - Cell lines
- METHOD DETAILS
 - Immunization of Tc bovine for production of anti-SARS-CoV-2 human polyclonal IgG
 - Neutralization assays
 - Preclinical Hamster model
 - Quantitative RT-PCR
- QUANTIFICATION AND STATISTICAL ANALYSIS

SUPPLEMENTAL INFORMATION

Supplemental information can be found online at <https://doi.org/10.1016/j.isci.2023.107764>.

ACKNOWLEDGMENTS

SAB Biotherapeutics, Inc., is receiving support from the Department of Defense Joint Program Executive Office for Chemical, Biological, Radiological, and Nuclear Defense (JPEO - CBRND) Joint Project Lead for Enabling Biotechnologies (JPL-EB), and from the Biomedical Advanced Research and Development Authority (BARDA), part of the Assistant Secretary for Preparedness and Response (ASPR) at the U.S. Department of Health and Human Services, to develop SAB-185, a countermeasure to SARS-CoV-2 (Effort sponsored by the U.S. Government under Other Transaction number W15QKN-16-9-1002 between the Medical CBRN Defense Consortium (MCDC), and the Government). The US Government is authorized to reproduce and distribute reprints for Governmental purposes notwithstanding any copyright notation thereon. The views and conclusions contained herein are those of the authors and should not be interpreted as necessarily representing the official policies or endorsements, either expressed or implied, of the U.S. Government. MDHA was supported by an NIH/NIAID T32 grant (T32 AI049820).

AUTHOR CONTRIBUTIONS

T.L., T.G., H.W., Z.W., D.R., and W.K. designed the experiments. Z.W., R.L., D.L., and D.R. produced the hACE2 hamsters. T.G., M.D., Y.T., M.A., S.V., J.L., D.R., and W.K. performed the experiments. T.G., M.D., T.L., H.W., C.B., K.E., E.S., and W.K. analyzed the data. W.K., T.G., and M.D. wrote the manuscript and T.L., H.W., Z.W., D.R., M.D., T.G., and W.K. edited the manuscript.

DECLARATION OF INTERESTS

H.W., T.L., C.B., K.E., and E.S. are employees of SAB Biotherapeutics and have financial interests. This work was supported by a contract from SAB Biotherapeutics, Inc., to the University of Pittsburgh (WK).

Received: April 18, 2023

Revised: July 24, 2023

Accepted: August 25, 2023

Published: August 29, 2023

REFERENCES

- Hu, B., Guo, H., Zhou, P., and Shi, Z.L. (2021). Characteristics of SARS-CoV-2 and COVID-19. *Nat. Rev. Microbiol.* 19, 141–154. <https://doi.org/10.1038/s41579-020-00459-7>.
- Plante, J.A., Mitchell, B.M., Plante, K.S., Debbink, K., Weaver, S.C., and Menachery, V.D. (2021). The variant gambit: COVID-19's next move. *Cell Host Microbe* 29, 508–515. <https://doi.org/10.1016/j.chom.2021.02.020>.
- Tegally, H., Wilkinson, E., Lessells, R.J., Giandhari, J., Pillay, S., Msomi, N., Mlisana, K., Bhiman, J.N., von Gottberg, A., Walaza, S., et al. (2021). Sixteen novel lineages of SARS-CoV-2 in South Africa. *Nat. Med.* 27, 440–446. <https://doi.org/10.1038/s41591-021-01255-3>.
- Kirby, T. (2021). New variant of SARS-CoV-2 in UK causes surge of COVID-19. *Lancet Respir. Med.* 9, e20–e21. [https://doi.org/10.1016/S2213-2600\(21\)00005-9](https://doi.org/10.1016/S2213-2600(21)00005-9).
- Zella, D., Giovanetti, M., Cella, E., Borsetti, A., Ciotti, M., Ceccarelli, G., D'Ettoire, G., Pezzuto, A., Tambone, V., Campanozzi, L., et al. (2021). The importance of genomic analysis in cracking the coronavirus pandemic. *Expert Rev. Mol. Diagn.* 21, 547–562. <https://doi.org/10.1080/14737159.2021.1917998>.
- Awadasseid, A., Wu, Y., Tanaka, Y., and Zhang, W. (2021). SARS-CoV-2 variants evolved during the early stage of the pandemic and effects of mutations on adaptation in Wuhan populations. *Int. J. Biol. Sci.* 17, 97–106. <https://doi.org/10.7150/ijbs.47827>.
- Groves, D.C., Rowland-Jones, S.L., and Agyal, A. (2021). The D614G mutations in the SARS-CoV-2 spike protein: Implications for viral infectivity, disease severity and vaccine design. *Biochem. Biophys. Res. Commun.* 538, 104–107. <https://doi.org/10.1016/j.bbrc.2020.10.109>.
- McCarthy, K.R., Rennick, L.J., Nambulli, S., Robinson-McCarthy, L.R., Bain, W.G., Haidar, G., and Duprex, W.P. (2021). Recurrent deletions in the SARS-CoV-2 spike glycoprotein drive antibody escape. *Science* 371, 1139–1142. <https://doi.org/10.1126/science.abf6950>.
- Kemp, S.A., Collier, D.A., Datt, R., Ferreira, I., Gayed, S., Jahun, A., Hosmillo, M., Rees-Spear, C., Mlcochova, P., Lumb, I.U., et al. (2020). Neutralising antibodies in Spike mediated SARS-CoV-2 adaptation. Preprint at medRxiv2020.12.05.20241927. <https://doi.org/10.1101/2020.12.05.20241927>.
- Hou, Y.J., Chiba, S., Halfmann, P., Ehre, C., Kuroda, M., Dinnon, K.H., 3rd, Leist, S.R., Schäfer, A., Nakajima, N., Takahashi, K., et al. (2020). SARS-CoV-2 D614G variant exhibits efficient replication ex vivo and transmission in vivo. *Science* 370, 1464–1468. <https://doi.org/10.1126/science.abe8499>.
- Gomez, C.E., Perdiguero, B., and Esteban, M. (2021). Emerging SARS-CoV-2 Variants and Impact in Global Vaccination Programs against SARS-CoV-2/covid-19. *Vaccines (Basel)* 9. <https://doi.org/10.3390/vaccines9030243>.
- Peacock, T.P., Penrice-Randal, R., Hiscox, J.A., and Barclay, W.S. (2021). SARS-CoV-2 one year on: evidence for ongoing viral adaptation. *J. Gen. Virol.* 102, 001584. <https://doi.org/10.1099/jgv.0.001584>.
- Plante, J.A., Liu, Y., Liu, J., Xia, H., Johnson, B.A., Lokugamage, K.G., Zhang, X., Muruato, A.E., Zou, J., Fontes-Garfias, C.R., et al. (2021). Spike mutation D614G alters SARS-CoV-2 fitness. *Nature* 592, 116–121. <https://doi.org/10.1038/s41586-020-2895-3>.
- Starr, T.N., Greaney, A.J., Dingens, A.S., and Bloom, J.D. (2021). Complete map of SARS-CoV-2 RBD mutations that escape the monoclonal antibody LY-CoV555 and its cocktail with LY-CoV016. *Cell Rep. Med.* 2, 100255. <https://doi.org/10.1016/j.xcrm.2021.100255>.
- Dejnirattisai, W., Shaw, R.H., Supasa, P., Liu, C., Stuart, A.S., Pollard, A.J., Liu, X., Lambe, T., Crook, D., Stuart, D.I., et al. (2022). Reduced neutralisation of SARS-CoV-2 omicron B.1.1.529 variant by post-immunisation serum. *Lancet* 399, 234–236. [https://doi.org/10.1016/S0140-6736\(21\)02844-0](https://doi.org/10.1016/S0140-6736(21)02844-0).
- VanBlargan, L.A., Errico, J.M., Halfmann, P.J., Zost, S.J., Crowe, J.E., Jr., Purcell, L.A., Kawaoka, Y., Corti, D., Fremont, D.H., and Diamond, M.S. (2022). An infectious SARS-CoV-2 B.1.1.529 Omicron virus escapes neutralization by therapeutic monoclonal antibodies. *Nat. Med.* 28, 490–495. <https://doi.org/10.1038/s41591-021-01678-y>.
- Cobey, S., Larremore, D.B., Grad, Y.H., and Lipsitch, M. (2021). Concerns about SARS-CoV-2 evolution should not hold back efforts to expand vaccination. *Nat. Rev. Immunol.* 21, 330–335. <https://doi.org/10.1038/s41577-021-00544-9>.
- Taylor, P.C., Adams, A.C., Hufford, M.M., de la Torre, I., Winthrop, K., and Gottlieb, R.L. (2021). Neutralizing monoclonal antibodies for treatment of COVID-19. *Nature Rev. Immunol.* 21, 382–393. <https://doi.org/10.1038/s41577-021-00542-x>.
- Focosi, D., and Maggi, F. (2021). Neutralising antibody escape of SARS-CoV-2 spike protein: Risk assessment for antibody-based Covid-19 therapeutics and vaccines. *Rev.*

- Med. Virol. 31, e2231. <https://doi.org/10.1002/rmv.2231>.
20. Kuroiwa, Y., Kasinathan, P., Sathiyaseelan, T., Jiao, J.A., Matsushita, H., Sathiyaseelan, J., Wu, H., Mellquist, J., Hammitt, M., Koster, J., et al. (2009). Antigen-specific human polyclonal antibodies from hyperimmunized cattle. *Nat. Biotechnol.* 27, 173–181. <https://doi.org/10.1038/nbt.1521>.
 21. Matsushita, H., Sano, A., Wu, H., Wang, Z., Jiao, J.A., Kasinathan, P., Sullivan, E.J., and Kuroiwa, Y. (2015). Species-Specific Chromosome Engineering Greatly Improves Fully Human Polyclonal Antibody Production Profile in Cattle. *PLoS One* 10, e0130699. <https://doi.org/10.1371/journal.pone.0130699>.
 22. Matsushita, H., Sano, A., Wu, H., Jiao, J.A., Kasinathan, P., Sullivan, E.J., Wang, Z., and Kuroiwa, Y. (2014). Triple immunoglobulin gene knockout transchromosomal cattle: bovine lambda cluster deletion and its effect on fully human polyclonal antibody production. *PLoS One* 9, e90383. <https://doi.org/10.1371/journal.pone.0090383>.
 23. Luke, T., Bennett, R.S., Gerhardt, D.M., Burdette, T., Postnikova, E., Mazur, S., Honko, A.N., Oberlander, N., Byrum, R., Ragland, D., et al. (2018). Fully Human Immunoglobulin G From Transchromosomal Bovines Treats Nonhuman Primates Infected With Ebola Virus Makona Isolate. *J. Infect. Dis.* 218, S636–S648. <https://doi.org/10.1093/infdis/jiy377>.
 24. Luke, T., Wu, H., Zhao, J., Channappanavar, R., Coleman, C.M., Jiao, J.A., Matsushita, H., Liu, Y., Postnikova, E.N., Ork, B.L., et al. (2016). Human polyclonal immunoglobulin G from transchromosomal bovines inhibits MERS-CoV in vivo. *Sci. Transl. Med.* 8, 326ra21. <https://doi.org/10.1126/scitranslmed.aaf1061>.
 25. Gardner, C.L., Sun, C., Luke, T., Raviprakash, K., Wu, H., Jiao, J.A., Sullivan, E., Reed, D.S., Ryman, K.D., and Klimstra, W.B. (2017). Antibody preparations from human transchromosomal cows exhibit prophylactic and therapeutic efficacy versus Venezuelan equine encephalitis virus. *J. Virol.* 91, e00226-17. <https://doi.org/10.1128/JVI.00226-17>.
 26. Liu, Z., Wu, H., Eglund, K.A., Gilliland, T.C., Dunn, M.D., Luke, T.C., Sullivan, E.J., Klimstra, W.B., Bausch, C.L., and Whelan, S.P.J. (2022). Human immunoglobulin from transchromosomal bovines hyperimmunized with SARS-CoV-2 spike antigen efficiently neutralizes viral variants. *Hum. Vaccines Immunother.* 18, 1940652. <https://doi.org/10.1080/21645515.2021.1940652>.
 27. Golden, J.W., Cline, C.R., Zeng, X., Garrison, A.R., Carey, B.D., Mucker, E.M., White, L.E., Shamblin, J.D., Brocato, R.L., Liu, J., et al. (2020). Human angiotensin-converting enzyme 2 transgenic mice infected with SARS-CoV-2 develop severe and fatal respiratory disease. *JCI Insight* 5, e142032. <https://doi.org/10.1172/jci.insight.142032>.
 28. Tang, J., Grubbs, G., Lee, Y., Wu, H., Luke, T.C., Eglund, K.A., Bausch, C.L., Sullivan, E.J., and Khurana, S. (2022). Increased antibody avidity and cross-neutralization of SARS-CoV-2 variants by hyperimmunized Tc-Bovine derived human immunoglobulins for treatment of COVID-19. *J. Infect. Dis.* 226, 655–663. <https://doi.org/10.1093/infdis/jiac031>.
 29. Muñoz-Fontela, C., Dowling, W.E., Funnell, S.G.P., Gsell, P.S., Riveros-Balta, A.X., Albrecht, R.A., Andersen, H., Baric, R.S., Carroll, M.W., Cavaleri, M., et al. (2020). Animal models for COVID-19. *Nature* 586, 509–515. <https://doi.org/10.1038/s41586-020-2787-6>.
 30. Damas, J., Hughes, G.M., Keough, K.C., Painter, C.A., Persky, N.S., Corbo, M., Hiller, M., Koepfli, K.P., Pfenning, A.R., Zhao, H., et al. (2020). Broad host range of SARS-CoV-2 predicted by comparative and structural analysis of ACE2 in vertebrates 117, 22311–22322. <https://doi.org/10.1073/pnas.2010146117>.
 31. Brooke, G.N., and Prischi, F. (2020). Structural and functional modelling of SARS-CoV-2 entry in animal models. *Sci. Rep.* 10, 15917. <https://doi.org/10.1038/s41598-020-72528-z>.
 32. Golden, J.W., Li, R., Cline, C.R., Zeng, X., Mucker, E.M., Fuentes-Lao, A.J., Spik, K.W., Williams, J.A., Twenhafel, N., Davis, N., et al. (2022). Hamsters Expressing Human Angiotensin-Converting Enzyme 2 Develop Severe Disease Following Exposure to SARS-CoV-2. *mBio* 0290621. <https://doi.org/10.1128/mbio.02906-21>.
 33. McCray, P.B., Jr., Pewe, L., Wohlford-Lenane, C., Hickey, M., Manzel, L., Shi, L., Netland, J., Jia, H.P., Halabi, C., Sigmund, C.D., et al. (2007). Lethal infection of K18-hACE2 mice infected with severe acute respiratory syndrome coronavirus. *J. Virol.* 81, 813–821. <https://doi.org/10.1128/JVI.02012-06>.
 34. Halfmann, P.J., Iida, S., Iwatsuki-Horimoto, K., Maemura, T., Kiso, M., Scheaffer, S.M., Darling, T.L., Joshi, A., Loeber, S., Singh, G., et al. (2022). SARS-CoV-2 Omicron virus causes attenuated disease in mice and hamsters. *Nature* 603, 687–692. <https://doi.org/10.1038/s41586-022-04441-6>.
 35. Hasanoglu, I., Korukluoglu, G., Asilturk, D., Cosgun, Y., Kalem, A.K., Altas, A.B., Kayaaslan, B., Eser, F., Kuzucu, E.A., and Guner, R. (2021). Higher viral loads in asymptomatic COVID-19 patients might be the invisible part of the iceberg. *Infection* 49, 117–126. <https://doi.org/10.1007/s15010-020-01548-8>.
 36. Nambulli, S., Xiang, Y., Tilston-Lunel, N.L., Rennick, L.J., Sang, Z., Klimstra, W.B., Reed, D.S., Crossland, N.A., Shi, Y., and Duprex, W.P. (2021). Inhalable Nanobody (PiN-21) prevents and treats SARS-CoV-2 infections in Syrian hamsters at ultra-low doses. *Sci. Adv.* 7, 432569. <https://doi.org/10.1101/2021.02>.
 37. Hartman, A.L., Nambulli, S., McMillen, C.M., White, A.G., Tilston-Lunel, N.L., Albe, J.R., Cottle, E., Dunn, M.D., Frye, L.J., Gilliland, T.H., et al. (2020). SARS-CoV-2 infection of African green monkeys results in mild respiratory disease discernible by PET/CT imaging and shedding of infectious virus from both respiratory and gastrointestinal tracts. *PLoS Pathog.* 16, e1008903. <https://doi.org/10.1371/journal.ppat.1008903>.
 38. Brocato, R.L., Kwilas, S.A., Kim, R.K., Zeng, X., Principe, L.M., Smith, J.M., and Hooper, J.W. (2021). Protective efficacy of a SARS-CoV-2 DNA vaccine in wild-type and immunosuppressed Syrian hamsters. *NPJ Vaccines* 6, 16. <https://doi.org/10.1038/s41541-020-00279-z>.
 39. Weisblum, Y., Schmidt, F., Zhang, F., DaSilva, J., Poston, D., Lorenzi, J.C., Muecksch, F., Rutkowska, M., Hoffmann, H.H., Michailidis, E., et al. (2020). Escape from neutralizing antibodies by SARS-CoV-2 spike protein variants. *Elife* 9, e61312. <https://doi.org/10.7554/eLife.61312>.
 40. Liu, Z., VanBlargan, L.A., Bloyet, L.M., Rothlauf, P.W., Chen, R.E., Stumpf, S., Zhao, H., Errico, J.M., Theel, E.S., Liebeskind, M.J., et al. (2021). Landscape analysis of escape variants identifies SARS-CoV-2 spike mutations that attenuate monoclonal and serum antibody neutralization. Preprint at bioRxiv. <https://doi.org/10.1101/2020.11.06.372037>.
 41. Asati, A., Kachurina, O., Karol, A., Dhir, V., Nguyen, M., Parkhill, R., Kouivaskaia, D., Chumakov, K., Warren, W., and Kachurin, A. (2016). Fluorescence Adherence Inhibition Assay: A Novel Functional Assessment of Blocking Virus Attachment by Vaccine-Induced Antibodies. *PLoS One* 11, e0144261. <https://doi.org/10.1371/journal.pone.0144261>.
 42. Klimstra, W.B., Tilston-Lunel, N.L., Nambulli, S., Boslett, J., McMillen, C.M., Gilliland, T., Dunn, M.D., Sun, C., Wheeler, S.E., Wells, A., et al. (2020). SARS-CoV-2 growth, furin-cleavage-site adaptation and neutralization using serum from acutely infected hospitalized COVID-19 patients. *J. Gen. Virol.* 101, 1156–1169. <https://doi.org/10.1099/jgv.0.001481>.
 43. Chi, X., Yan, R., Zhang, J., Zhang, G., Zhang, Y., Hao, M., Zhang, Z., Fan, P., Dong, Y., Yang, Y., et al. (2020). A neutralizing human antibody binds to the N-terminal domain of the Spike protein of SARS-CoV-2. *Science* 369, 650–655. <https://doi.org/10.1126/science.abc6952>.

STAR★METHODS

KEY RESOURCES TABLE

REAGENT or RESOURCE	SOURCE	IDENTIFIER
Antibodies		
Human anti-SARS-CoV-2 plasma panel	NIBSC	20/120
Human anti-SARS-CoV-2 plasma panel	NIBSC	20/130
Tc Bovine-derived human anti-SARS-CoV-2 IgG	SAb Biotherapeutics	SAb-185
Bacterial and virus strains		
SARS-CoV-2/München-1.1/2020/929	Klimstra et al., 2020 ⁴²	N/A
SARS-Related Coronavirus 2, Isolate hCoV-19/England/204820464/2020	BEI Resources	Cat# NR-54000
SARS-Related Coronavirus 2, Beta Isolate hCoV-19/South Africa/KRISP-K005325/2020	BEI Resources	Cat# NR-54009
SARS-Related Coronavirus 2, Gamma Isolate hCoV-19/Japan/TY7-503/2021 (Brazil P.1)	BEI Resources	Cat# NR-54982
SARS-Related Coronavirus 2, Delta Isolate hCoV-19/USA/CA-VRLC086/2021 (lineage AY.1)	BEI Resources	Cat# NR-55691
SARS-related Coronavirus 2, Omicron isolate hCoV-19/USA/CO-CDPHE-2102544747/2021(lineage BA.2-B.1.1.529)	BEI Resources	Cat# NR-56522
SARS-Related Coronavirus 2 Omicron isolate (lineage BA.2.12.1)	BEI Resources	Cat# NR-56782
NIAID, NIH SARS-Related Coronavirus 2 Omicron isolate (lineage BA.4)	BEI Resources	Cat# NR-56803
SARS-Related Coronavirus 2 Omicron isolate hCoV-19/USA/COR-22-063113/2022 (lineage BA.5)	BEI Resources	Cat# NR-58616
SARS-CoV-2 D144-146 virus (4 aa deletion in NTR RDR 2)	McCarthy, K.R. et al., 2021 ⁸ Chi, X. et al., 2020 ⁴³	N/A
Chemicals, peptides, and recombinant proteins		
Immunodiffusion Agarose	MP Biomedicals	Cat# 952012
Crystal Violet	Fisher Scientific	Cat# C581
Opti-MEM	Gibco	Cat# 31985-070
DMEM	Corning	Cat# 10-013-CV
Fetal Bovine Serum	R&D Systems	Cat# S12450
L-Glutamine	Corning	Cat# 25-005-CI
Penicillin Streptomycin	Corning	Cat# 30-002-CI
Sodium Pyruvate	Corning	Cat# 25-000-CI
Puromycin	Mirus Bio	Cat# MIR5940
Isoflurane	Covetrus	Cat# 29405
TRIzol Reagent	Invitrogen/Thermo Fisher	Cat# 15596018
PBS, 1X	Corning	Cat# 21-031-CV
Critical commercial assays		
Reliance One-Step Multiplex Supermix	Bio-Rad	Cat# 12010176
20 x 18s rRNA Control Mix	Applied Biosystems	Cat# 4318839
Experimental models: Cell lines		
VERO E6 C1008	ATCC	Cat# CRL-1586
VERO E6-TMPRSS2-T2A-ACE2	BEI Resources	Cat# NR-54970

(Continued on next page)

Continued

REAGENT or RESOURCE	SOURCE	IDENTIFIER
<i>Experimental models: Organisms/strains</i>		
Golden Syrian Hamster	Charles River	Cat# LVG
hACE-2 Golden Syrian Hamster	Dr. Zhongde Wang, Utah State University	N/A
<i>Oligonucleotides</i>		
nCOV_N2 Forward Primer Aliquot, 100 nmol (5' TTA CAA ACA TTG GCC GCA AA 3')	IDTdna	Cat# 100006833
nCOV_N2 Reverse Primer Aliquot, 100 nmol (5' GCG CGA CAT TCC GAA GAA 3')	IDTdna	Cat# 100006834
nCOV_N2 Probe Aliquot, 50 nmol (5' 6-FAM/ACA ATT TGC CCC CAG CGC TTC AG/BHQ_1 3')	IDTdna	Cat# 100006835
<i>Software and algorithms</i>		
GraphPad Prism	https://www.graphpad.com/	N/A
CLC Genomics Workbench	https://digitalinsights.qiagen.com/products-overview/discovery-insights-portfolio/analysis-and-visualization/qiagen-clc-genomics-workbench/	N/A

RESOURCE AVAILABILITY**Lead contact**

Further information is available by request and should be directed to Dr. William Klimstra (Klimstra@pitt.edu).

Materials availability

Full genotypes of unpassaged viral stocks are available at <https://www.beiresources.org>.

(NIBSC product information sheets available at <https://www.NIBSC.org>)

The creation and characterization of the SAB-185 human polyclonal IgG is an SAB Biotherapeutics IP and is restricted. Please contact Dr. Thomas Luke (tluke@sab.bio) with inquiries.

Data and code availability

- Data reported in this paper will be shared by the [lead contact](#) upon request.
- The paper does not report any original code.
- Any additional information required to reanalyze the data reported in this paper is available from the [lead contact](#) upon request.

EXPERIMENTAL MODEL AND STUDY PARTICIPANTS DETAILS**Animals***Tc bovine*

Adult Tc bovine of mixed sex used in this study are homozygous for triple knockout in the endogenous bovine immunoglobulin genes (*IGHM* – /– *IGHML1* – /– *IGL* – /–). Briefly, both bovine immunoglobulin heavy-chain (*bIGH*) loci were homozygously inactivated by gene targeting.²⁰ Because lambda light chain (*bIGL*) is the predominantly expressed light-chain isotype in bovine B cells, homozygous inactivation of the *bIGL* locus was performed by deleting the entire bovine lambda gene cluster.²² To reconstitute B cell function in Tc bovine, a human artificial chromosome (HAC) was used. The HAC is comprised of a human chromosome 14 fragment which contains the entire unrearranged germline loci of human immunoglobulin heavy chain (*hIGH*). In addition, the HAC includes the human chromosome 2 fragment containing the entire human immunoglobulin K light chain locus (*hIGK*).²¹ To further enhance fully human IgG production with human IgG1 subclass dominance in Tc bovine, the human *IGHM* constant region and key regulatory sequences on the HAC were optimized.^{21,41}

Syrian Golden and hACE-2 transgenic hamsters

Male and female hACE2 hamsters of 8–14 weeks of age were obtained from Utah State University and male and female normal Syrian hamsters between 8 and 12 weeks of age were purchased from Charles River. All animals were randomized by animal support staff and housed singly after receipt at the University of Pittsburgh. All hamster procedures were in accordance with AAALAC procedures and approved by the University of Pittsburgh IACUC committee (protocol #IS00017405).

Viral stocks

The Munich strain (containing D614G) was obtained and amplified in Vero E6 cells (ATCC CRL-1586) as described,⁴² while the Alpha, Beta, Gamma, Delta and Omicron viruses were obtained from BEI Resources [BEI Resources, NIAID, NIH: SARS-Related Coronavirus 2, Isolate hCoV-19/England/204820464/2020, NR-54000, contributed by Bassam Hallis; BEI Resources, NIAID, NIH: SARS-Related Coronavirus 2, Beta Isolate hCoV-19/South Africa/KRISP-K005325/2020, NR-54009, contributed by Alex Sigal and Tulio de Oliveira; BEI Resources, NIAID, NIH: SARS-Related Coronavirus 2, Gamma Isolate hCoV-19/Japan/TY7-503/2021 (Brazil P.1), NR-54982, contributed by National Institute of Infectious Diseases; BEI Resources, NIAID, NIH: SARS-Related Coronavirus 2, Delta Isolate hCoV-19/USA/CA-VRLC086/2021 (lineage AY.1), NR-55691, contributed by Andrew S. Pekosz; BEI resources, NIAID, NIH SARS-related Coronavirus 2, Omicron isolate hCoV-19/USA/CO-CDPHE-2102544747/2021, NR-56522, (lineage BA.2-B.1.1.529); contributed by Centers for Disease Control and Prevention; BEI Resources, NIAID, NIH: SARS-Related Coronavirus 2 Omicron isolate, NR-56782 (lineage BA.2.12.1) contributed by Dr. Viviana Simon; BEI Resources, NIAID, NIH SARS-Related Coronavirus 2 Omicron isolate, NR-56803 (lineage BA.4) contributed by Dr. Andrew S. Pekosz; BEI Resources, NIAID, NIH: SARS-Related Coronavirus 2 Omicron isolate hCoV-19/USA/COR-22-063113/2022 (lineage BA.5), NR-58616, contributed by Dr. Richard J. Webby, respectively]. The D144-146 virus (4 aa deletion in NTR RDR 2) was obtained from an immunocompromised patient as described and removes an epitope recognized by mAb 4A8.^{8,43} The Munich (D614G; 4.0 x 10⁶ Vero E6 PFU/ml) and D 141–144 (5.0 x 10⁵ Vero E6 PFU/ml) viruses were isolates passaged two times in Vero E6 cells and shown to possess an intact S protein furin protease cleavage signal.^{8,42} The Alpha (4.0 x 10⁶ Vero E6 PFU/ml), Beta (9.5 x 10⁶ Vero E6 PFU/ml), Gamma (6.8x10⁶ Vero E6 PFU/ml) and Omicron (BA.2-B.1.1.529 [6.5 x 10⁵ Vero A/T pfu/ml] BA.2-B.2.12.1 [1.3 x 10⁷ Vero A/T pfu/ml], BA.4 [Vero A/T 3.6 x 10⁶ pfu/mL] and BA.5 [1.2 x 10⁷ Vero A/T pfu/ml]), viruses were unamplified stocks from BEI Resources, diluted and used directly. The Delta and Omicron BA.2-B.1.1.529 variants (Delta 6.8 x 10⁶ Vero E6 PFU/ml; Omicron 1.5 x 10⁴ Vero E6 PFU/ml) were obtained from BEI resources and passaged one time in Vero hACE2/TMPRSS2 cells (BEI Resources, NIAID, NIH: *Cercopithecus aethiops* Kidney Epithelial Cells Expressing Transmembrane Protease, Serine 2 and Human Angiotensin-Converting Enzyme 2 (Vero E6-TMPRSS2-T2A-ACE2, NR-54970). The passaged Gamma and Delta variants were deep-sequenced (Illumina, MiGS sequencing center, Pittsburgh, PA) and no differences with the BEI isolates were found in the structural protein regions.

Cell lines

Vero E6 cells

African green monkey kidney Vero C1008, Clone E6 (ATCC CRL-1586) cells were cultured in DMEM (Corning) 10% FBS (R&D Systems), 1 mM L-Glutamine (Corning), 1x penicillin/streptomycin (Corning) in a humidified incubator with 5% CO₂ at 37C.

Vero E6-TMPRSS2-T2A-ACE2

Stably transfected African green monkey kidney Vero E6-TMPRSS2-T2A-ACE2 (BEI Resources NR-54970) cells were cultured in DMEM (Corning) 10% FBS (R&D Systems), 1 mM L-Glutamine (Corning), 0.75 mg/mL Sodium Bicarbonate (Corning), 10ug/mL Puromycin (Mirus Bio) in a humidified incubator with 5% CO₂ at 37C. For neutralization assays, cells were maintained in the regular Vero E6 growth media as described in this paper.

METHOD DETAILS

Immunization of Tc bovine for production of anti-SARS-CoV-2 human polyclonal IgG

Tc Bovine were vaccinated, plasma collected and purified as described previously.²⁶ Briefly, Tc bovines were immunized twice with plasmid DNA expressing the Wuhan WA-1 strain spike protein at three-week intervals. Starting week six, animals were boosted three times with recombinant WA-1 spike ectodomain protein derived from insect cells. Plasma from weeks 7–8, 11–12 and 15–16 were pooled and human IgG was purified for the SAB-185 final preparation. Tc bovine plasma was thawed, pooled, fractionated by caprylic acid (CA), and clarified by depth filtration in the presence of Celpure P1000 filter aid. The clarified sample containing Tc bovine-derived human IgG is further purified by affinity chromatography, first using an anti-human IgG kappa light chain-specific column, KappaSelect (GE Healthcare Life Sciences) to capture hIgG followed by a low pH treatment, and second, by passing through an anti-bovine IgG heavy chain-specific affinity column, Capto HC15 (GE Healthcare Life Sciences). To further remove residual IgG that contains bovine heavy chain, the human IgG fraction was then subjected to a Q Sepharose chromatography polishing step to further reduce impurities, nanofiltration, final buffer exchange, concentration, and sterile filtration. Finally, the SAB-185 product was terminally filtered and filled into vials.

Neutralization assays

Neutralization capacity of SAB-185 and the NIBSC convalescent serum controls (NIBSC 20/130 and 20/120) was assayed by Vero E6 or Vero hAce2/TMPRSS2 cells (grown in DMEM [Corning], 10% FBS [R&D Systems], 1 mM L Glutamine [Corning], 1x penicillin/streptomycin [Corning]) plaque neutralization assay. Due to unavailability of additional NIBSC 20/130, we used NIBSC 20/120 (from the 20/118 panel) for the Delta variant neutralizations (NIBSC product information sheets available at <https://www.NIBSC.org>). NIBSC 20/120 was used at a similar live SARS CoV-2 PRNT₅₀ concentration to NIBSC 20/130 and NIBSC 20/120 PRNT₅₀ and PRNT₈₀ endpoints were calculated for the Munich virus for comparison. SAB-185 was diluted to 1 mg/ml in PBS and then diluted serially 2-fold before reaction with viruses, while the NIBSC controls were diluted 2-fold directly from NIBSC vials. All Ab samples were heat inactivated by incubation at 56°C for 30 min. Viruses were diluted in

OPTI-MEM (Gibco) with 2% FBS to approximately 200 PFU in 250 μ L and reacted with an equal volume of serial 2-fold dilutions of each antibody (in PBS) for 1 h at 37°C followed by infection of Vero E6 monolayers for 1 h at 37°C. A solution of 0.1% immunodiffusion agarose (MP Bio) in 2X Vero E6 growth medium was then added and plaques were developed at 37°C for 72–96 h followed by removal of agarose, staining of cells with crystal violet (Fisher Scientific) and counting of plaques. At least three independent dilutions of each sample were performed, and these were replicated in two averaged wells per dilution. Data points represent averages of the three independent dilutions.

Preclinical Hamster model

Equal numbers of male and female hACE2 Hamsters of 8–14 weeks of age (4–10/group) were given either a 50 mg/kg dose of SAb185 (treated) diluted in PBS or 50 μ L of PBS (control) in the gastrocnemius muscle. Twenty-four hours later, all hamsters were challenged intratracheally (it.) with 50 μ L of virus diluent (OPTIMEM medium; Gibco) containing 1000 Vero E6 or Vero hAce2/TMPRSS2 cell plaque-forming units of each virus. For comparison of intratracheal and intranasal routes of infection hACE 2 hamsters were infected with 1000 PFU it. Or 100 PFU intranasally by instillation of 25 μ L of diluted virus into each nostril. Normal Syrian Hamsters (Charles River) of random sex between 8 and 12 weeks of age were challenged it. with 1000 PFU of the Munich strain. We observed a sex-based difference with several variants in the hACE2 model with control group females uniformly succumbing to infection with each tested virus, but males exhibited approximately 50–100% mortality depending upon the experiment.

Hamsters were observed (~30 seconds-1 minute) twice daily post challenge through day 12 (acute viral disease period). Animals were assessed for the appearance of signs of disease: ruffled fur, hunching, increased respiratory rate, anorexia or lethargy, and scored accordingly (0 for no, 1 for yes) with a cumulative number totaled for the clinical score. Data is presented as the inverse of the clinical score sum values to be comparable to weight loss data. For oropharyngeal swabs, animals were sedated with isoflurane (3–5%) and a sterile swab was inserted into the oral cavity and upper trachea and then placed into virus diluent. Quantitative RT-PCR and plaque assays were performed on RNA purified from plasma and swab supernatants or directly with plaque assay. Weights were recorded once daily. Hamsters losing >20% of starting body weight or exhibiting prolonged hunching/ataxia (>3 days) indicative of severe disease were euthanized.

Quantitative RT-PCR

One step quantitative RT-PCR was performed as previously described⁴² for SARS CoV-2 RNA on blood or from oropharyngeal swabs taken at multiple times post challenge. Quantitative RT-PCR primer/probe sets (forward 5' TTA CAA ACA TTG GCC GCA AA 3', reverse 5' GCG CGA CAT TCC GAA GAA 3' probe: 5' 6-FAM/ACA ATT TGC CCC CAG CGC TTC AG/BHQ_1 3') were directed to the nucleocapsid gene in region of conserved sequence between the variant viruses. Virus isolation/titration was also performed with the samples using Vero E6 cells using a standard SARS CoV-2 plaque assay as described.⁴²

QUANTIFICATION AND STATISTICAL ANALYSIS

Results were evaluated for statistical significance with GraphPad PRISM software. Mortality curves were evaluated using Mantel-Cox Log Rank analysis. Average weight loss, clinical sign and virus titration data were compared with two-way ANOVA. Individual time points in particular assays were compared between two treatments with a two-tailed Student's *t* test. Neutralization data was analyzed and PRNT₅₀/PRNT₈₀ calculated using Graphpad PRISM and the asymmetric sigmoidal 5PL standard curve fit (confidence limit 95%).